IET Nanobiotechnology

Research Article

IET Journals
The Institution of Engineering and Technology

Facile synthesis by a covalent binding reaction for pH-responsive drug release of carboxylated chitosan coated hollow mesoporous silica nanoparticles

ISSN 1751-8741
Received on 23rd April 2017
Revised 16th November 2017
Accepted on 13th December 2017
E-First on 28th February 2018
doi: 10.1049/iet-nbt.2017.0100
www.ietdl.org

Qiang Liu[1], Jiao Wang[1], Linnan Yang[1], Xiaofei Xia[1], Mei Wang[1], Shengguang Chen[2], Rongrong Zhu[1], Qingxiu Wang[1], Xianzheng Wu[2], Shilong Wang[1] ✉

[1]*Research Center for Translational Medicine at East Hospital, School of Life Science and Technology, Tongji University, Shanghai, People's Republic of China*

[2]*Tongji Hospital, Tongji University, Shanghai, People's Republic of China*

✉ *E-mail: wsl@tongji.edu.cn*

Abstract: In this study, a promising drug nano-carrier system consisting of mono-dispersed and pH sensitive carboxylated chitosan-hollow mesoporous silica nanoparticles (Ccs-HMSNs) suitable for the treatment of malignant cells was synthesised and investigated. At neutral pH, the Ccs molecules are orderly aggregated state, which could effectively hinder the release of loaded drug molecules. However, in slightly acidic environment, Ccs chains are heavily and flexibly entangled in gel state, which would enhance the subsequent controlled release of the loaded drug. Using doxorubicin hydrochloride (DOX•HCl) as the drug model, their results demonstrated that the system had an excellent loading efficiency (64.74 μg/mg Ccs-HMSNs) and exhibited a pH-sensitive release behaviour. Furthermore, confocal laser scanning microscopy revealed that the Ccs-HMSNs nanocomposite could effectively deliver and release DOX•HCl to the nucleus of HeLa cells, thereby inducing apoptosis. In addition, MTT assay also confirmed that DOX•HCl loaded Ccs-HMSNs (DOX•HCl@Ccs-HMSNs) exhibited a good anticancer effect on HeLa cells with a time-dependent manner. Finally, haemolysis experiment showed Ccs-HMSNs had no haemolytic activity at all the tested concentrations (5–320 μg/mL). Thus, this biocompatible and effective nano-carrier system will have potential applications in controllable drug delivery and cancer therapy.

1 Introduction

Over the past few decades, nanoparticles have been developed for application as drug carriers to deliver therapeutic agents into targeted cells or organs [1–3]. Among them, mesoporous silica nanoparticles (MSNs) are one of the most promising candidates owing to its remarkable properties, including favourable biocompatibility, facile synthesis, large surface area, excellent chemical stability, unique mesoporous structure, as well as easy functionalisation and chemical inertness [4–6]. Thus, numerous efforts have been devoted to the development of MSNs-related drug delivery systems. For instance, polymer-coated mesoporous silica nanoparticles were exploited for pH-triggering drug delivery [7]. In another study, chitosan was capped onto the surfaces of MSNs to achieve pH-responsive nanocarriers [8–11]. In these theranostic systems, polymer-coated MSNs can improve drug solubility and targeting, provide controlled release of the therapeutics into the targeted tumour tissues or the blood stream, and prolong the circulation time of drugs [12]. Hollow mesoporous silica nanoparticles (HMSNs), with a unique large hollow cavity inside each original MSN, are ideal as new-generation drug delivery systems with extraordinarily high loading capacity. In comparison with MSNs, HMSNs have greater potential in diverse applications, including the facts that (i) the interstitial hollow cavities can serve as reservoirs to store cargo or as nanoreactors to support chemical reactions, (ii) mesopores enable the cargo to diffuse through the intact shell [13]. In particular, when the pores in the HMSNs shell were tuned, such a drug delivery system could combine the merits of hollow interior/large surface area/high pore volume for efficient drug encapsulation, and tunable pore sizes for controlled drug delivery [14]. In addition, foreign material depositions in vivo are reduced due to need lower amount of HMSNs to achieve desired therapeutic effect comparing with that of MSNs. Therefore, HMSNs have received increasing interests, and many research studies on HMSNs employed as drug delivery system have been reported. For example, Shen *et al.* reported that HMSNs were used to encapsulate bortezomib so as to improve its efficacy for non-small cell lung cancer therapy [15]. However, some issues need to be further overcome.

On one hand, just as MSNs, burst release of anticancer agents is one of the well-documented disadvantages of unmodified HMSNs [16, 17]. On the other hand, silica materials are known to cause the haemolysis of mammalian red blood cells (RBCs) [8, 18]. So, it is essential to improve their biocompatibility and minimise the toxicity of anticancer drugs so as to enhance the therapeutic efficacy. Like the conventional bare MSNs [19, 20], the above shortages will be overcome and the nanoparticles will be highly desirable in clinical applications when the surface of the HMSNs can be conjugated with specific ligands that are stimuli-responsive.

According to the stimuli previously studies, pH-responsive drug delivery systems have received particular attention for cancer therapies because cancer tissues exhibit lower pH values compared with normal cells [21–23]. Carboxylated chitosan (Ccs) is an important chitosan derivative synthesised by the partial substitution of carboxyl groups onto hydroxyl groups and amino groups. Apart from favourable biodegradability and excellent biocompatibility, Ccs possess a high water solubility. Meanwhile, the carboxyl groups in its structure can make it react with other molecules easily through graft polymerisation [24]. So, it can be extensively used in different drug delivery and biomedical applications [25, 26]. In addition, the amino groups in Ccs would be protonated at a certain pH range, which indicates the Ccs can be responsive to an external pH-stimuli. Hence, Ccs may serve as a promising biopolymer that provides HMSNs with a pH responsive polyelectrolyte layer to control the release of entrapped therapeutic agents to the acidic local environment in cancer tissues.

In this work, we report a straightforward and facile fabrication of carboxylated chitosan-grafted hollow mesoporous silica nanoparticles (Ccs-HMSNs) through a covalent binding reaction, and demonstrate that the fabricated nanocarriers can efficiently

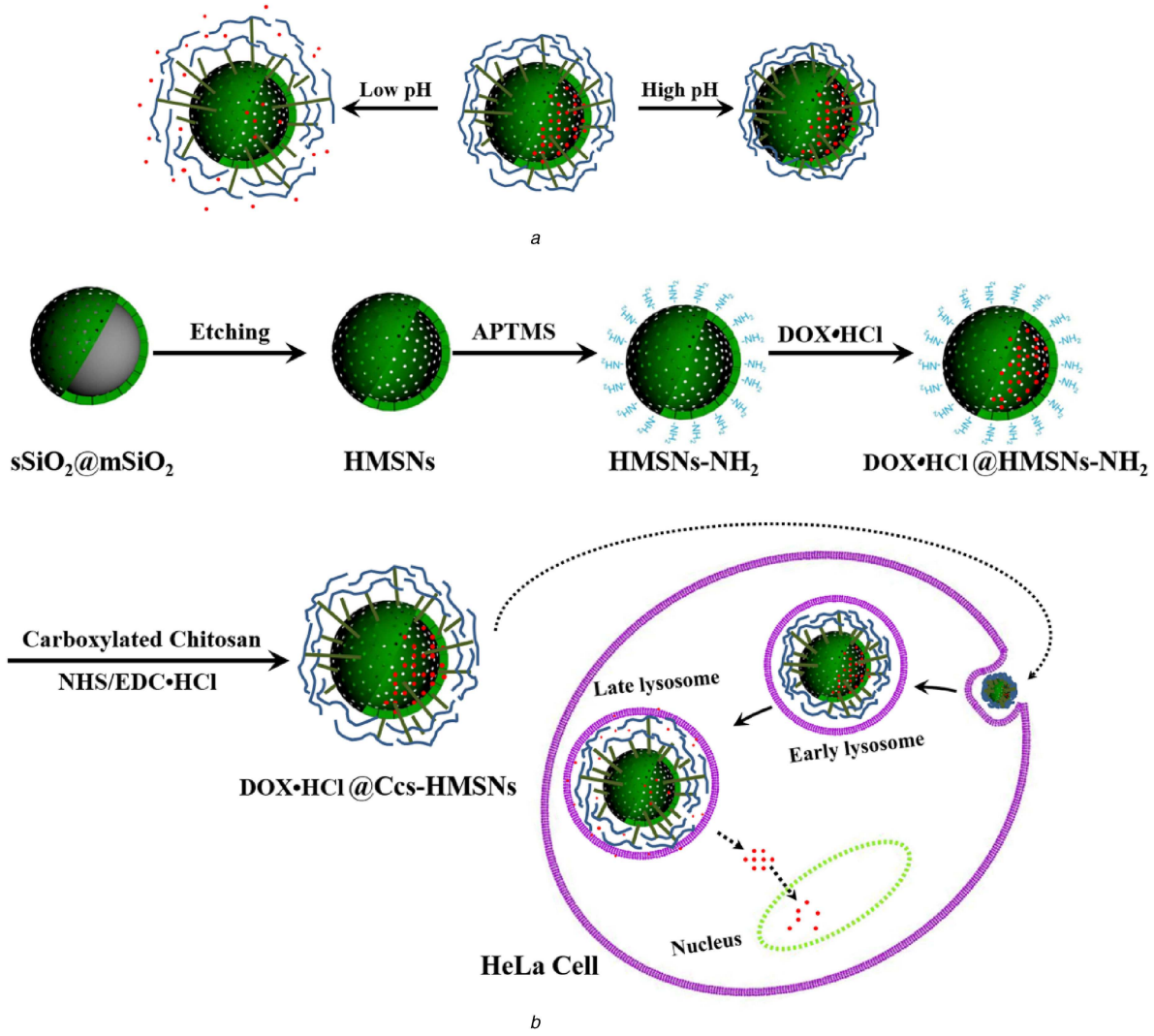

Fig. 1 *Schematic illustration*

(a) Drug release from Ccs-HMSNs at different pH values, ***(b)*** Synthesis of DOX•HCl@Ccs-HMSNs-based pH controlled-release system and controlled release of DOX•HCl at lysosome (or endosome) inside HeLa cells

load anticancer drugs and tailor the release of drug molecules under different pH conditions (Fig. 1). In this core-shell structured nanoparticles, a hollow mesoporous silica nanoparticle acts as the drug loading core, and the carboxylated chitosan serves as the gating shell. Furthermore, the loading and controlled-release ability of the Ccs-HMSNs was studied using a classic anticancer drug, doxorubicin hydrochloride (DOX•HCl), as the model. In addition, the cellular internalisation and cytotoxicity of DOX•HCl@Ccs-HMSNs were investigated. Finally, the biocompatibility of Ccs-HMSNs was explored through haemolysis assay.

2 Materials and methods

2.1 Materials

Tetraethylorthosilicate (TEOS), octadecyltrimethoxysilane (C18TMS), dimethylsulfoxide (DMSO), 3-aminopropyltrimethoxysilane (APTMS), *N*-(3-dimethylaminopropyl)-*N*′-ethylcarbodiimide hydrochloride (EDC•HCl), and *N*-hydroxysuccinimide (NHS) were purchased from Aladdin Chemistry Co. Ltd. (Shanghai, China). Ccs with a carboxylation degree (≥60%) and viscosity (10–80 mPa s) was purchased from Amresco (Solon, OH, USA). Absolute ethanol, aqueous ammonia (28 wt%), and sodium carbonate (Na_2CO_3) were purchased from Sinopharm Chemical Reagent Co., Ltd. (Shanghai, China). Doxorubicin hydrochloride (DOX•HCl, purity ≥ 98%) was purchased from Shanghai Hualan Chemical Co., Ltd. (Shanghai, China). 3-(4,5-Dimethylthiazol-2-yl)-2,5-diphenyltetrazolium bromide (MTT) was purchased from Sigma-Aldrich Co. (St Louis, MO, USA). 2-(4-Amidinophenyl)-6-indolecarbamidine dihydrochloride (DAPI) was purchased from KeyGen Biotech Co., Ltd. (Nanjing, China). Dulbecco's modified Eagle's medium (DMEM) and foetal calf serum (FCS) were purchased from HyClone (Logan, UT, USA). All chemicals were of analytical grade and were used without further purification. Deionised water with a resistivity of 18.2 MΩ/cm produced by a Milli-Q water system was used in all the experiments.

Cell culture: HeLa cells were cultured at 37°C in flasks containing DMEM and 10% FCS in a humidified atmosphere and 5% CO_2 in a Thermo culturist (Thermo Fisher; Waltham, MA, USA).

2.2 Synthesis of HMSNs

The synthesis of HMSNs was performed using a Na_2CO_3-etching method according to the previously published reports [14, 27]. Briefly, 71.4 mL of absolute ethanol was mixed with 10 mL of deionised water and 3.14 mL of aqueous ammonia, then the solution was stirred for 10–20 min at 30°C. Subsequently, 6 mL of TEOS was added to the above mixture under vigorous stirring, and the reaction lasted for 1 h. After that, 5 mL of TEOS and 3 mL of C_{18}TMS were sufficiently premixed and added into the reaction medium rapidly, and the reaction lasted for another 1 h. Furthermore, the nanoparticles collected by centrifugation which served as the solid silica core/mesoporous silica shell nanospheres (designated as $sSiO_2@mSiO_2$) were dispersed into Na_2CO_3 aqueous solution (0.6 M), which was etched under constant stirring

for 6 h at 80°C. The resultant was centrifuged, washed with deionised water and ethanol, and dried in a vacuum oven at 55°C for 24 h to yield the as-prepared HMSNs. Finally, uniform HMSNs were obtained after the calcination of the as-prepared products in air at 550°C for 6 h.

2.3 Synthesis of HMSNs-NH_2 and Ccs-HMSNs

To functionalise the HMSN surface with $–NH_2$ groups, 0.2 g of HMSNs was first dispersed in 40 mL of absolute ethanol, followed by addition of 0.5 mL of APTMS. After being stirred at room temperature for 24 h, the mixture was extensively washed with absolute ethanol and dried in a vacuum oven at 55°C to obtain the aminated HMSNs (HMSNs-NH_2). Next, Ccs was covalently conjugated onto HMSNs-NH_2 through the –COOH group by using cross-linking reagents EDC•HCl and NHS. Specifically, 0.02 g of Ccs was dissolved in 4 mL of deionised water followed by the addition of 0.02 g of EDC•HCl and 0.04 g of NHS. The mixture was then stirred at room temperature for 15 min to activate the carboxylic group of Ccs. Subsequently, 0.05 g of the prepared MSNs-NH_2 powder well dispersed in 5 mL of deionised water was added to the above solution, and the mixture was stirred for 24 h at room temperature. Finally, Ccs-HMSNs were obtained by centrifugation, washing three times with deionised water, and freeze-drying using a tabletop lyophiliser.

2.4 Characterisation

Transmission electron microscopy (TEM) images were obtained on a JEM 1230 transmission electron microscope (JEOL 1230; JEOL, Tokyo, Japan). Scanning electron microscopy (SEM) images were obtained on a S-4800 scanning electron microscope (Hitachi, Tokyo, Japan). Zeta potential measurements were carried out on a Malvern NanoZS 90 zetasizer (Malvern Instruments, Malvern, UK). Fourier transform infrared (FTIR) absorption spectra were recorded on a Nicolet Nexus 470 spectrometer (Nicolet; Madison, WI, USA). An X-ray diffraction (XRD) pattern was recorded on an X-ray diffractometer (D8 Advance; Bruker Corporation, Billerica, MA, USA) using CuKα irradiation ($\lambda = 0.154$ nm). Nitrogen adsorption–desorption isotherms were measured at 77 K on a Micromeritics TriStar 3000 analyser (Micromeritics, Norcross, GA, USA). The surface areas were calculated using the Brunauer–Emmett–Teller (BET) model, and the pore-size distributions were calculated using the Barrett–Joyner–Halenda (BJH) model.

2.5 Drug loading

Two major steps were involved in the preparation of DOX•HCl loaded Ccs-HMSNs (DOX•HCl@Ccs-HMSNs). Firstly, 0.1 g of HMSNs-NH_2 was dispersed in 25 mL of 0.5 mg/mL DOX·HCl water solution at pH 7.5. After the mixture was stirred for 24 h in the dark, HMSNs loaded with DOX•HCl (denoted as DOX•HCl@HMSNs-NH_2) were centrifuged and washed with 20 mL of deionised water for three times. Then, DOX•HCl@HMSNs-NH_2 were freeze-dried in a tabletop lyophiliser. Secondly, the Ccs was capped onto the surface of DOX•HCl@HMSNs-NH_2 to produce the DOX•HCl@Ccs-HMSNs through the same method in synthesis of Ccs-HMSNs. The amount of DOX•HCl loaded into the HMSNs-NH_2 and Ccs-HMSNs was determined by subtracting the mass of DOX•HCl in the supernatant from the total mass of DOX•HCl determined by UV–vis spectroscopy at 480 nm.

2.6 Drug release

The in vitro release patterns of DOX•HCl from the Ccs-HMSNs were studied using the dialysis membrane method [28]. Briefly, two batches of DOX•HCl@Ccs-HMSNs (50 mg) were suspended in a phosphate-buffered saline (PBS) solution (10 mL) at respective pH values of 7.4 and 6.0, shaking at 100 rpm (37°C). At fixed time intervals, 2 mL of solution was withdrawn from the beaker, and the same volume of fresh corresponding buffer was added to the original suspension. For the measurement of DOX•HCl release amount, the absorbance of the release medium at 480 nm was recorded on a Cary 50 UV–vis spectrophotometer (Varian, Palo Alto, CA, USA). Besides, in vitro pH-responsive release behaviour of the Ccs-HMSNs in cancer cells (HeLa) was investigated according to previously reported procedures [29]. Briefly, HeLa cells were seeded into glass bottom dishes (In Vitro Scientific, Sunnyvale, CA, USA) at a density of 2×10^5 cells per dish and incubated for 24 h. Subsequently, cells were treated with DOX•HCl@HMSNs, DOX•HCl@HMSNs-NH_2, and DOX•HCl@Ccs-HMSNs at DOX•HCl concentration of 10 μg/mL for 3 h. To investigate the intracellular release efficiency, the culture media containing excess nano-carriers were discarded and replaced by 2 mL of pH 6.0 and pH 7.4 buffer solution. After the cells were further incubated for 30 min, the buffer solutions were discarded, and the cells were washed thrice with PBS (pH 7.4) to remove excess nanoparticles. The cells were fixed with 4% paraformaldehyde (1 mL) for 10 min at room temperature and stained with DAPI (0.2 μg/mL) in methanol for 15 min at 37°C. Then, the cells were observed with a confocal laser scanning microscope (FV1000 Fluoview; Olympus Corporation).

2.7 Cellular uptake study

To demonstrate efficient cellular uptake, HeLa cells were seeded into glass bottom dishes (In Vitro Scientific, Sunnyvale, CA, USA) at a density of 2×10^5 cells per dish and incubated for 24 h. Then the cells were incubated with free DOX•HCl and DOX•HCl@Ccs-HMSNs (DOX•HCl concentration at 1 μg/mL) in the culture medium at 37°C for 1, 4, 12, 24 and 48 h, respectively, followed by three washes with PBS (pH 7.4). After that, the cells were fixed with 4% paraformaldehyde (1 mL) for 10 min at room temperature and stained with DAPI (0.2 μg/mL) in methanol for 15 min at 37°C. Finally, the cells were viewed and imaged as above in the part of in vitro drug release.

2.8 Cytotoxicity of Ccs-HMSNs and DOX•HCl@Ccs-HMSNs

Cell viability was evaluated using a standard MTT assay, as described previously [30]. Briefly, HeLa cells were seeded at 8000 cells per well into 96-well plates and incubated for 24 h. Then the original culture media were replaced with 100 μL of fresh growth media containing Ccs-HMSNs or DOX•HCl@Ccs-HMSNs at the indicated concentrations. The incubation continued for 24, 48, 72, or 96 h. A group without treatment under the same conditions was served as control. After treatment, 20 μL MTT PBS(5 mg/mL) was added and incubated for another 4 h. Then, the culture medium was removed and 150 μL DMSO was added. Finally, absorbance was monitored at 492 nm by using an ELx800 reader (BioTek Instruments, Inc., Winooski, VT, USA).

2.9 Haemolysis assay

The assay experiment was carried out according to a previous report [18]. 0.8 mL of the PBS solutions of HMSNs and Ccs-HMSNs were added into 0.2 mL of diluted RBCs suspension, respectively, and the final concentrations of the nanoparticles were 5, 10, 20, 40, 80, 160, and 320 μg/mL. Incubation of deionised water and PBS with RBCs were served as positive and negative controls, respectively. The mixed solutions were then vortexed and kept in static conditions at room temperature for 2 h. Subsequently, all the samples were centrifuged at 12,000*g* at 4°C for 5 min, and the absorbance values of the supernatants at 541 nm were measured using a UV–vis spectrophotometer.

3 Results

3.1 Synthesis and characterisation of HMSNs and Ccs-HMSNs

From SEM and TEM images in Figs. 2*a* and *d*, HMSNs presented monodispersed spherical morphology and uniform hollow nanostructure, which the average particle size is around 200 nm. However, after the modification of amino groups, the morphology of the HMSNs was not changed (Figs. 2*b* and *e*). As shown in Figs. 2*c* and *f*, a clear thin layer as indicated by a white arrow could

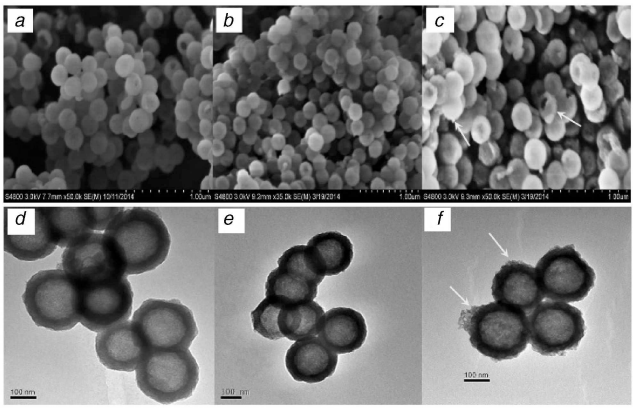

Fig. 2 *SEM images*
(a) HMSNs, ***(b)*** HMSNs-NH_2, and ***(c)*** Ccs-HMSNs, respectively. TEM images of ***(d)*** HMSNs, ***(e)*** HMSNs-NH_2, and ***(f)*** Ccs-HMSNs, respectively

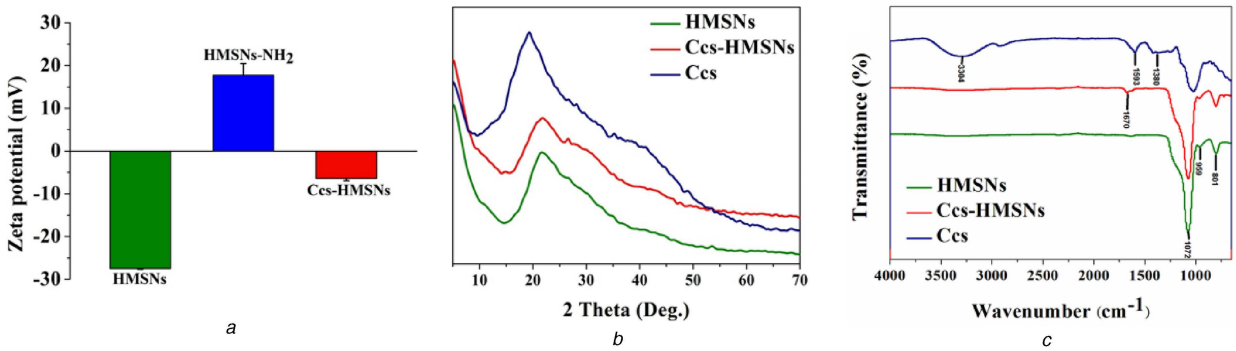

Fig. 3 *Verification of the surface modification of HMSNs*
(a) Zeta potential distribution of HMSNs, HMSNs-NH_2 and Ccs-HMSNs in PBS solution, ***(b)*** XRD pattern of HMSNs, Ccs-HMSNs, and Ccs, ***(c)*** FTIR spectra of HMSNs, Ccs-HMSNs, and Ccs

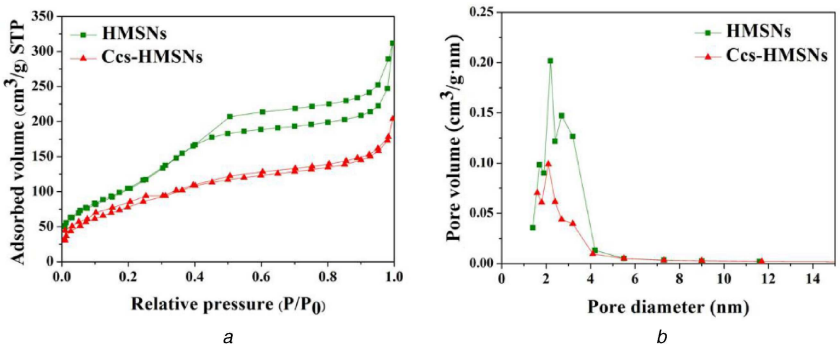

Fig. 4 *Analysis of mesoporous structures*
(a) BET N_2 adsorption–desorption isotherm of HMSNs and Ccs-HMSNs, ***(b)*** BJH pore size distribution of HMSNs and Ccs-HMSNs

be seen on the surface of the Ccs-HMSNs, indicating the existence of the Ccs conjugated on the HMSNs.

The surface modification of HMSNs has been also studied by zeta potential, XRD, and FTIR analysis (Figs. 3*a*–*c*). As shown in Fig. 3*a*, the mean zeta potential of HMSNs, HMSNs-NH_2, and Ccs-HMSNs was −27.5, 17.8, and −6.4 mV, respectively, consistent with the modification of amine groups (HMSNs-NH_2) on the negatively charged silica surface (HMSNs) and subsequent conjugation of Ccs on the positively charged HMSNs-NH_2. Due to the carboxy groups of Ccs would be ionised at pH ≃ 7.0, Ccs-HMSNs are negatively charged. The results of XRD pattern showed that Ccs-HMSNs was complex of Ccs crystallise and HMSNs (Fig. 3*b*). As indicated in Fig. 3*c*, unmodified HMSNs displayed strong absorption signals at 801, 959, and 1085 cm^{-1}, which were assigned to the symmetric stretching Si–O–Si, stretching vibrations of Si–OH, and asymmetric stretching Si–O–Si, respectively [31]. The Ccs revealed typical peaks of 1380 cm^{-1} (amide III) [7], 1593 cm^{-1} (amide II) [7] and 3304 cm^{-1} (–OH of carboxyl). However, after the modification of Ccs, the emergence of a new peak at 1670 cm^{-1} is attributed to the amide carbonyl (CO–NH bond) stretching vibration [32].

The nitrogen adsorption–desorption technique further demonstrated that the synthesised HMSNs possessed mesoporous structures. As shown in Fig. 4, the HMSNs achieved exhibit typical Langmuir IV hysteresis loops, indicating the existence of well-defined mesopores. The BET surface area, total pore volume, and pore diameter of the HMSNs were 393.69 m^2/g, 0.48 cm^3/g, and 3.51 nm, respectively. While, after being conjugation with Ccs, these parameters were changed to 296.35 m^2/g, 0.31 cm^3/g, and 2.21 nm, respectively (Table 1).

3.2 Drug loading and release evaluation

To evaluate drug loading efficiency and pH-responsive drug release behaviour of Ccs-HMSNs, DOX•HCl, a model drug, was preloaded into HMSNs-NH_2 as described in 2.5 *Drug loading*. According to the experimental parameters and calculation method,

Table 1 Structural parameters of HMSNs and Ccs-HMSNs

Samples	BET surface area, m^2/g	Total pore volume, cm^3/g	Pore diameter, nm
HMSNs	393.69	0.48	3.51
Ccs-HMSNs	296.35	0.31	2.21

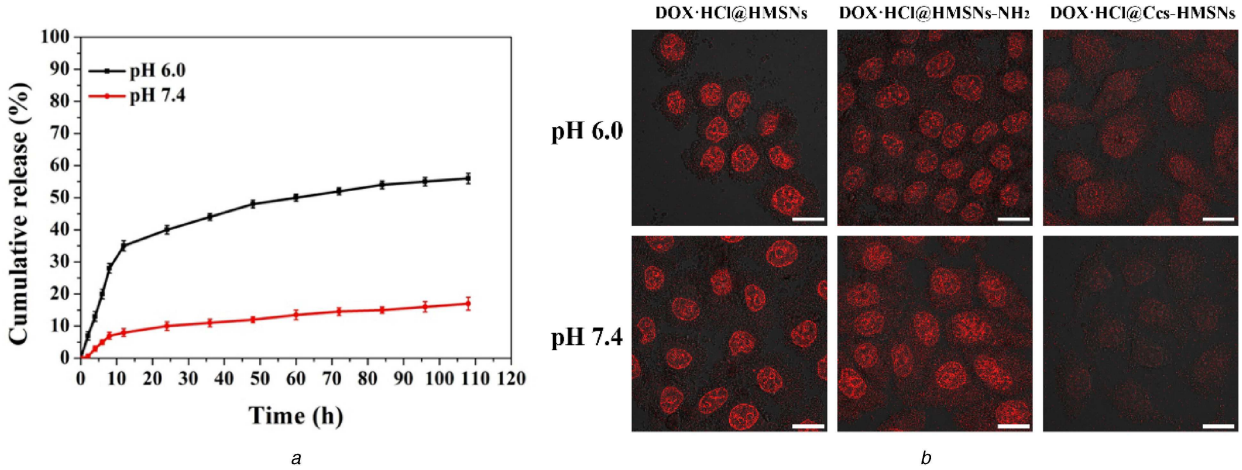

Fig. 5 *In vitro release profile of DOX•HCl@Ccs-HMSNs*
(a) DOX•HCl release profiles of the DOX•HCl@Ccs-HMSNs at pH 6.0 and 7.4. Results shown as mean ± standard deviation ($n = 3$), ***(b)*** Fluorescence images of HeLa cells incubated with DOX•HCl@HMSNs, DOX•HCl@ HMSNs-NH_2, and DOX•HCl@Ccs-HMSNs at pH 6.0 and pH 7.4 for 30 min, respectively. Red colour is for DOX•HCl. Scale bars are 20 μm

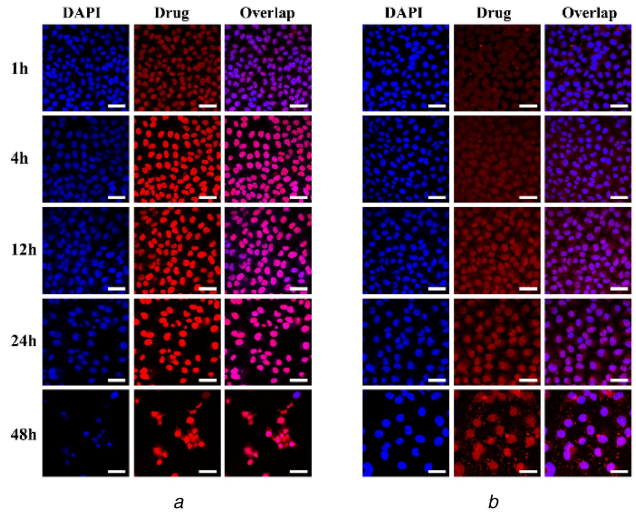

Fig. 6 *CLSM images of HeLa cells after incubation with 1 μg/mL*
(a) Free DOX•HCl and ***(b)*** DOX•HCl@Ccs-HMSNs for 1, 4, 12, 24, and 48 h, respectively. Left: blue colour is for nuclear stain DAPI, middle: red colour is for DOX•HCl, right: overlap of the left and middle images. Scale bars are 50 μm

the absolute drug loading content was 78.20 and 64.74 μg/mg for HMSNs-NH_2 and Ccs-HMSNs, respectively.

To investigate the pH-dependent releasing characteristics, DOX•HCl@Ccs-HMSNs were dispersed in PBS buffer solutions at different pHs (6.0 and 7.4) at 37°C. As shown in Fig. 5*a*, the released amount of DOX•HCl increased with the decrease of pH. Under physiological pH condition (7.4), only about 17% of DOX•HCl was released over 108 h. In contrast, at pH 6.0, the released amount of DOX•HCl from DOX•HCl@Ccs-HMSNs system remarkably increased to about 56%, more than three times that at pH 7.4. Besides, to further evaluate the in vitro pH-responsive release behaviour of the drug delivery system, HeLa cells were used as the model cancer cells, and the procedure was depicted in the Experimental Section. In this experiment, to confirm that DOX•HCl@Ccs-HMSNs have the pH-dependent releasing characteristics, the in vitro drug release of DOX•HCl@HMSNs and DOX•HCl@HMSNs-NH_2 were also explored. Briefly, HeLa cells were incubated with DOX•HCl@HMSNs, DOX•HCl@HMSNs-NH_2, and DOX•HCl@Ccs-HMSNs at DOX•HCl concentration of 10 μg/mL for 3 h. Then, 2 mL of pH 6.0 and pH 7.4 buffer solution was, respectively, added to replace the original cell culture medium, followed by the cells were further incubated for 30 min. As shown in Fig. 5*b*, obviously, the intracellular fluorescence of DOX•HCl under pH 6.0 was stronger than that under pH 7.4 in the group incubated with DOX•HCl@Ccs-HMSNs. However, as expected, no obvious fluorescence intensity change was found in DOX•HCl@HMSNs and DOX•HCl@HMSNs-NH_2 at different pH conditions, such as pH 6.0 or 7.4, and the fluorescence intensity of the cell nuclei in both the groups were stronger than that DOX•HCl@Ccs-HMSNs group at the same pH conditions, indicating that DOX•HCl was faster and easier to release from DOX•HCl@HMSNs and DOX•HCl@HMSNs-NH_2.

3.3 Cellular uptake of DOX•HCl@Ccs-HMSNs

To prove that the released DOX•HCl from the DOX•HCl@Ccs-HMSNs could be further delivered into the cell nuclei, the cellular uptake and distribution of the released DOX•HCl in HeLa cells was further investigated. The cell nuclei were labelled with blue-fluorescent DAPI as an indicator. As shown in Fig. 6, the intracellular DOX•HCl delivery from both the DOX•HCl formulations exhibited the similar profiles in HeLa cells but at different time points, which was consistent with previous report [11]. Free DOX•HCl could rapidly and easily enter into HeLa cells and accumulated in the cell nuclei by diffusion within 1 h of incubation, and the intensive drug fluorescence could be observed inside the cell nuclei after 4 h of incubation. For DOX•HCl@Ccs-HMSNs; however, the drug fluorescence was initially more located in the cytoplasm of the perinuclear area after incubation for 1 h, followed by appeared and became more intense in the nucleus with increasing incubation time. Besides, with increasing incubation time, the cells incubated with free DOX•HCl and DOX•HCl@Ccs-HMSNs in visual fields were both decreased.

3.4 In vitro cytotoxicity studies

The cytotoxicity of Ccs-HMSNs was investigated to examine their in vitro biocompatibility. Cell proliferation was assessed using HeLa cells and an MTT assay. As shown in Fig. 7*a*, no obvious cytotoxic effects were observed when the cells were treated with a

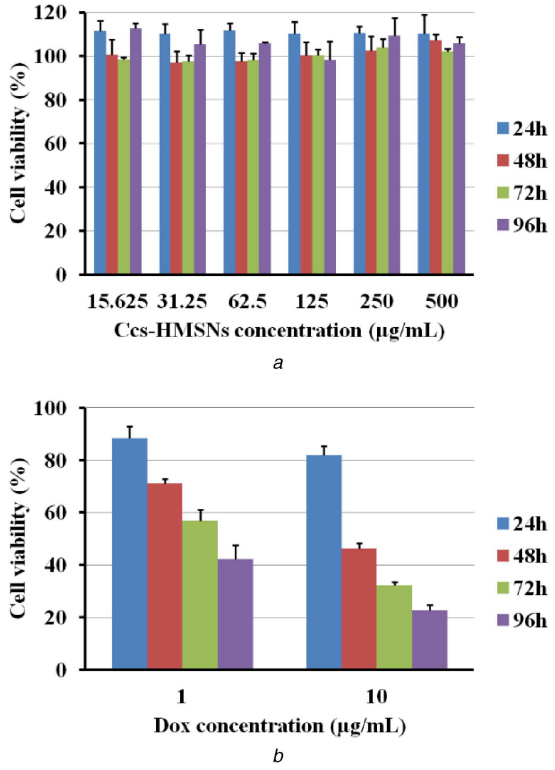

Fig. 7 *MTT assay*

(a) Viability of HeLa cells incubated with concentrations of Ccs-HMSNs from 15.625 to 500 μg/mL for 24, 48, 72, and 96 h, ***(b)*** Viability of HeLa cells treated with DOX•HCl@Ccs-HMSNs (concentration of DOX•HCl was 1 and 10 μg/mL, respectively) for 24, 48, 72, and 96 h. The error bars represent means of six independent experiments

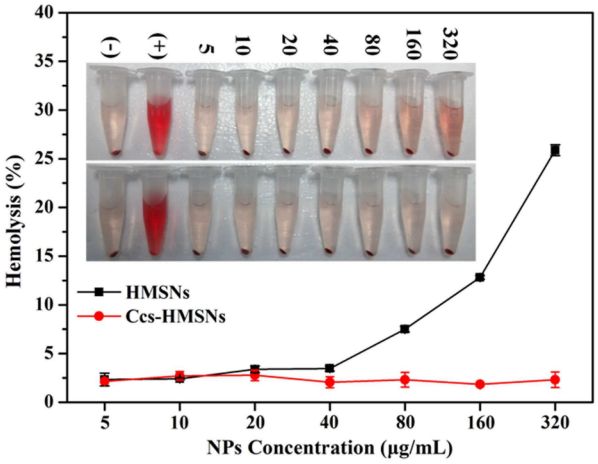

Fig. 8 *Haemolysis assay of HMSNs and Ccs-HMSNs samples*

series of Ccs-HMSNs solutions at different concentrations (15.625–500 μg/mL) for 24, 48, 72, and 96 h, respectively.

Subsequently, the cytotoxicity of DOX•HCl@Ccs-HMSNs on HeLa cells was also evaluated. As shown in Fig. 7*b*, when HeLa cells were treated with DOX•HCl@Ccs-HMSNs at different DOX concentrations (1 and 10 μg/mL) for 24, 48, 72, and 96 h, respectively, the dose-dependent cytotoxicity on the cell was observed. Furthermore, DOX•HCl@Ccs-HMSNs showed prolonged cytotoxicity to HeLa cells over a longer period of 96 h.

3.5 Haemolytic behaviour of HMSNs and Ccs-HMSNs

To evaluate the in vivo biocompatibility of Ccs-HMSNs, a haemolysis assay was carried out. The result of haemolysis assay was shown in Fig. 8. As shown in Fig. 8, the optical images presented the direct observation of haemolysis at different nanoparticle concentrations (5, 10, 20, 40, 80, 160, and 320 μg/mL) of HMSNs and Ccs-HMSNs, respectively. It can be seen that the haemolysis effect becomes visible at the increased concentrations of HMSNs. Especially, when the concentration of HMSNs reached 320 μg/mL, the colour change of the resulting solution was obvious compared with the negative control. However, as expected, no visible haemolysis effect can be observed visually treated with Ccs-HMSNs. To further determine the RBCs' haemolysis effect, the absorbance of the supernatant at 541 nm was measured by UV–vis spectroscopy. In Fig. 8, when the concentration of HMSNs reached 160 and 320 μg/mL, the percentage haemolysis was 12.82 and 25.87%, respectively. However, as expected, Ccs-HMSNs showed no haemolytic effect on RBCs.

4 Discussion

Hollow mesoporous silica nanoparticles (HMSNs) have been extensively investigated as a drug delivery system because of its remarkable properties. Some issues in the process of its practical application, however, need to be further overcome. The obstacles include interaction between the silane groups on the surface of HMSNs and some biological molecules during the circulation, and undesirable premature drug release before the HMSNs-based delivery systems reach and enter the cancerous cells. In this study, Ccs was applied to cover the pores of HMSNs with covalent bonds as the ''gatekeeper'' to overcome aforementioned problems. Moreover, compared with other similar reports about MSNs and HMSNs-based drug delivery systems, the design and synthesis of our formulation (DOX•HCl@Ccs-HMSNs) in this study was straightforward and facile, as well as time-saving.

SEM and TEM images shown a clear thin layer can be seen on the surface of the fabricated Ccs-HMSNs, indicating the existence of the Ccs conjugated on the HMSNs, which was further confirmed by the evidence of the N_2 adsorption and desorption measurements. In comparison to HMSNs without surface functionalisation, the specific surface area, pore volume and pore diameter of Ccs-HMSNs were reduced, which were consistent with the results previously reported in [10, 33]. The surface area, pore volume and pore diameter of HMSNs were 393.69 m^2/g, 0.48 cm^3/g, and 3.51 nm, respectively. After being coating with Ccs, these parameters were reduced to 296.35 m^2/g, 0.31 cm^3/g, and 2.21 nm, respectively. This result suggested that that the pore openings of the HMSNs were indeed coated by Ccs. In addition, we speculate that Ccs was easier to form a pH-responsive protection layer on the outer surface of the fabricated DOX•HCl@Ccs-HMSNs, because DOX•HCl was firstly loaded into the hollow cavities and mesoporous channels of HMSNs-NH_2. When DOX•HCl@Ccs-HMSNs was resuspended in PBS (7.4), the DOX•HCl release percent was very low (<20%), while the corresponding release percent in PBS (6.0) was ~3.3-fold as that of in PBS (7,4), indicating the good controlled release property of Ccs as the gatekeepers. Consistent with our expectations, by conjugating Ccs on HMSNs, the fabricated Ccs-HMSNs were endowed with a pH-responsive release capability. This postulation would further draw support from the intracellular fluorescence intensity and the phenomenon that were observed with a confocal laser scanning microscope. Based on these results, it can also be demonstrated that DOX•HCl@Ccs-HMSNs possess a pH-sensitive releasing behaviour. Besides, the cellular uptake result demonstrated that the DOX•HCl@Ccs-HMSNs initially were endocytosed into the cells and released the DOX•HCl within the cytosol, followed by diffusion into the nuclei, resulting in a prolonged and slower DOX•HCl accumulation in the nuclei.

The MTT and the haemolysis data collected from the current study demonstrated that the blank nano-carriers showed good biocompatibility and were suitable for use as drug delivery systems. Moreover, the MTT assay also revealed that DOX•HCl@Ccs-HMSNs exhibited a dose-dependent and time-dependent cytotoxicity on HeLa cells. As we know, in the physiological environment, HMSNs could cause haemolysis phenomenon which limited its biomedical applications in vivo. In the process of haemolysis, haemoglobin will be released from the RBCs into solution, which leads the resulting solution to be visually red. It is beyond doubt that the high degree of haemolysis

raised serious safety concerns in the term of the application of HMSNs as drug delivery. Some explanations for the haemolytic effect have been proposed, including the generation of reactive oxygen species induced by the surface of the silica [34], the high affinity of silanol group of silica for binding with tetra-alkyl ammonium groups that are abundant in RBCs membranes [18, 35] and denaturation of membrane proteins through electrostatic interactions with (–SiO–) groups at the silica surface [36]. However, modification of the Ccs on the surface of HMSNs can significantly reduce the generation of ROS, and the affinity between the tetra-alkyl ammonium groups and HMSNs, as well as the electrostatic interactions between membrane proteins and groups at the silica surface. In this work, when the surface of HMSNs was modified with Ccs, the resulting Ccs-HMSNs showed no haemolytic effect on RBCs, indicating Ccs can improve the biocompatibility of HMSNs when administered intravenously, which improved the clinical application of HMSNs. Looking to the future, many issues, such as distribution and anti-tumour efficacy of DOX•HCl@Ccs-HMSNs in vivo, need to be systematically investigated.

5 Conclusion

In summary, we have successfully developed a novel pH-sensitive nanocomposite-based drug delivery system consisting of hollow mesoporous silica nanoparticles capped with Ccs (Ccs-HMSNs). It was constructed with simplicity of design and easy of synthesis. In this study, DOX•HCl, a commonly used anticancer drug, was selected as the drug model. It was presented that the Ccs-HMSNs system had a high loading amount of drug (64.74 μg/mg Ccs-HMSNs) and good pH-triggered release behaviour. Besides, the images captured by confocal laser scanning microscopy revealed that Ccs-HMSNs nanocomposite could effectively deliver and release DOX•HCl to the nucleus of HeLa cells, thereby inducing apoptosis. In addition, DOX•HCl@Ccs-HMSNs demonstrated obvious cytotoxicity towards HeLa cells with a dose and time-dependent manner. Finally, the good biocompatibility of Ccs-HMSNs was confirmed by haemolysis experiment. Thus, a simple, highly effective, and pH-responsive nanocomposite has been demonstrated, which can serve as a promising anticancer drug carrier for clinical applications.

6 Acknowledgments

This work was financially supported by the National Natural Science Foundation of China (grant nos. 31570849, 81671105), the National Key Research and Development Program (grant no. 2016YFA0100800), and the Fundamental Research Funds for the Central Universities.

7 References

[1] Peng, H.B., Li, K., Wang, T., *et al.*: 'Preparation of hierarchical mesoporous CaCO3 by a facile binary solvent approach as anticancer drug carrier for etoposide', *Nanoscale Res. Lett.*, 2013, **8**, (1), pp. 321–331

[2] Wang, J., Zhu, R.R., Sun, X.Y., *et al.*: 'Intracellular uptake of etoposide-loaded solid lipid nanoparticles induces an enhancing inhibitory effect on gastric cancer through mitochondria-mediated apoptosis pathway', *Int. J. Nanomed.*, 2014, **9**, pp. 3987–3998

[3] Pathania, D., Gupta, D., Kothiyal, N.C., *et al.*: 'Preparation of a novel chitosan-g-poly(acrylamide)/Zn nanocomposite hydrogel and its applications for controlled drug delivery of ofloxacin', *Int. J. Biol. Macromol.*, 2016, **84**, pp. 340–348

[4] Xiang, D., Lin, H., Guo, W., *et al.*: 'Simple way to obtain pH-sensitive drug release from functional mesoporous silica materials', *IET Nanobiotechnol.*, 2014, **8**, (4), pp. 179–183

[5] Wang, J., Zhu, R.R., Gao, B., *et al.*: 'The enhanced immune response of hepatitis B virus DNA vaccine using SiO_2@LDH nanoparticles as an adjuvant', *Biomaterials*, 2014, **35**, (1), pp. 466–478

[6] Vivero-Escoto, J.L., Elnagheeb, M.: 'Mesoporous silica nanoparticles loaded with cisplatin and phthalocyanine for combination chemotherapy and photodynamic therapy in vitro', *Nanomaterials*, 2015, **5**, (4), pp. 2302–2316

[7] Tang, H.Y., Guo, J., Sun, Y., *et al.*: 'Facile synthesis of pH sensitive polymer-coated mesoporous silica nanoparticles and their application in drug delivery', *Int. J. Pharmcol.*, 2011, **421**, (2), pp. 388–396

[8] Hu, X.X., Wang, Y., Peng, B.: 'Chitosan-capped mesoporous silica nanoparticles as pH-responsive nanocarriers for controlled drug release', *Chem. Asian J.*, 2014, **9**, (1), pp. 319–327

[9] Popat, A., Liu, J., Lu, G.Q.M., *et al.*: 'A pH-responsive drug delivery system based on chitosan coated mesoporous silica nanoparticles', *J. Mater. Chem.*, 2012, **22**, pp. 11173–11178

[10] Chen, F., Zhu, Y.C.: 'Chitosan enclosed mesoporous silica nanoparticles as drug nano-carriers: sensitive response to the narrow pH range', *Micropor. Mesopor. Mater.*, 2012, **150**, pp. 83–89

[11] Feng, W., Nie, W., He, C., *et al.*: 'Effect of pH-responsive alginate/chitosan multilayers coating on delivery efficiency, cellular uptake and biodistribution of mesoporous silica nanoparticles based nanocarriers', *ACS Appl. Mater. Interfaces*, 2014, **6**, (11), pp. 8447–8460

[12] Liu, S., Maheshwari, R., Kiick, K.L.: 'Polymer-based therapeutics', *Macromolecules*, 2009, **42**, (1), pp. 3–13

[13] Li, Y., Li, N., Pan, W., *et al.*: 'Hollow mesoporous silica nanoparticles with tunable structures for controlled drug delivery', *ACS Appl. Mater. Interfaces*, 2017, **9**, (3), pp. 2123–2129

[14] Gao, Y., Chen, Y., Ji, X.F., *et al.*: 'Controlled intracellular release of doxorubicin in multidrug-resistant cancer cells by tuning the shell-pore sizes of mesoporous silica nanoparticles', *ACS Nano*, 2011, **5**, (12), pp. 9788–9798

[15] Shen, J., Song, G.S., An, M., *et al.*: 'The use of hollow mesoporous silica nanospheres to encapsulate bortezomib and improve efficacy for non-small cell lung cancer therapy', *Biomaterials*, 2014, **35**, (1), pp. 316–326

[16] Slowing, I.I., Vivero-Escoto, J.L., Wu, C.W., *et al.*: 'Mesoporous silica nanoparticles as controlled release drug delivery and gene transfection carriers', *Adv. Drug Deliv. Rev.*, 2008, **60**, (11), pp. 1278–1288

[17] Xing, L., Zheng, H.Q., Cao, Y.Y., *et al.*: 'Coordination polymer coated mesoporous silica nanoparticles for pH-responsive drug release', *Adv. Mater.*, 2012, **24**, (48), pp. 6433–6437

[18] Slowing, I.I., Wu, C.W., Vivero-Escoto, J.L., *et al.*: 'Mesoporous silica nanoparticles for reducing hemolytic activity towards mammalian red blood cells', *Small*, 2009, **5**, (1), pp. 57–62

[19] Zheng, Q.S., Lin, T.R., Wu, H.Y., *et al.*: 'Mussel-inspired polydopamine coated mesoporous silica nanoparticles as pH-sensitive nanocarriers for controlled release', *Int. J. Pharm.*, 2014, **463**, (1), pp. 22–26

[20] Hu, X.X., Hao, X.H., Wu, Y., *et al.*: 'Multifunctional hybrid silica nanoparticles for controlled doxorubicin loading and release with thermal and pH dually response', *J. Mater. Chem. B Mater. Biol. Med.*, 2013, **1**, (8), pp. 1109–1118

[21] Schmaljohann, D.: 'Thermo- and pH-responsive polymers in drug delivery', *Adv. Drug Deliv. Rev.*, 2006, **58**, (15), pp. 1655–1670

[22] Dong, J.Y., Xue, M., Zink, J.I.: 'Functioning of nanovalves on polymer coated mesoporous silica nanoparticles', *Nanoscale*, 2013, **5**, (21), pp. 10300–10306

[23] Zou, Z., He, D.G., He, X.X., *et al.*: 'Natural gelatin capped mesoporous silica nanoparticles for intracellular acid-triggered drug delivery', *Langmuir*, 2013, **29**, (41), pp. 12804–12810

[24] Harish Prashanth, K.V., Tharanathan, R.N.: 'Studies on graft copolymerization of chitosan with synthetic monomers', *Carbohydr. Polym.*, 2003, **54**, (3), pp. 343–351

[25] Wang, H., Song, F.L., Chen, Q., *et al.*: 'Antitumor and antimetastasis effects of macerating solutions from an injectable chitosan-based hydrogel on hepatocarcinoma', *J. Biomed. Mater. Res. A*, 2015, **103**, (12), pp. 3879–3885

[26] Deng, Z., Zhen, Z., Hu, X., *et al.*: 'Hollow chitosan-silica nanospheres as pH-sensitive targeted delivery carriers in breast cancer therapy', *Biomaterials*, 2011, **32**, (21), pp. 4976–4986

[27] Chen, F., Hong, H., Shi, S.X., *et al.*: 'Engineering of hollow mesoporous silica nanoparticles for remarkably enhanced tumor active targeting efficacy', *Sci. Rep.*, 2014, **4**, pp. 5080–5089

[28] Zhang, P., Wu, T., Kong, J.L.: 'In situ monitoring of intracellular controlled drug release from mesoporous silica nanoparticles coated with pH-responsive charge-reversal polymer', *ACS Appl. Mater. Interfaces*, 2014, **6**, (20), pp. 17446–17453

[29] Wu, X., Wang, Z.Y., Zhu, D., *et al.*: 'Ph and thermo dual-stimuli-responsive drug carrier based on mesoporous silica nanoparticles encapsulated in a copolymer-lipid bilayer', *ACS Appl. Mater. Interfaces*, 2013, **5**, (21), pp. 10895–10903

[30] Wang, J., Zhu, R.R., Sun, D.M., *et al.*: 'Intracellular uptake of curcumin-loaded solid lipid nanoparticles exhibit anti-inflammatory activities superior to those of curcumin through the NF-κB signaling pathway', *J. Biomed. Nanotechnol.*, 2015, **11**, (3), pp. 403–415

[31] Gangwar, R.K., Tomar, G.B., Dhumale, V.A., *et al.*: 'Curcumin conjugated silica nanoparticles for improving bioavailability and its anticancer applications', *J. Agric. Food Chem.*, 2013, **61**, (40), pp. 9632–9637

[32] Yu, M.H., Jambhrunkar, S., Thorn, P., *et al.*: 'Hyaluronic acid modified mesoporous silica nanoparticles for targeted drug delivery to CD44-overexpressing cancer cells', *Nanoscale*, 2013, **5**, (1), pp. 178–183

[33] Zhang, Y., Ang, C.Y., Li, M., *et al.*: 'Polymer-coated hollow mesoporous silica nanoparticles for triple-responsive drug delivery', *ACS Appl. Mater. Interfaces*, 2015, **7**, (32), pp. 18179–18187

[34] Nash, T., Allison, A.C., Harington, J.S.: 'Physico-chemical properties of silica in relation to its toxicity', *Nature*, 1966, **210**, (5033), pp. 259–261

[35] Depasse, J., Warlus, J.J.: 'Relation between the toxicity of silica and its affinity for tetraalkylammonium groups. comparison between $Si0_2$ and $Ti0_2$', *Colloid Interface Sci.*, 1976, **56**, (3), pp. 618–621

[36] Diociaiuti, M., Bordi, F., Gataleta, L., *et al.*: 'Morphological and functional alterations of human erythrocytes induced by SiO_2 particles: An electron microscopy and dielectric spectroscopy study', *Environ. Res.*, 1999, **80**, (3), pp. 197–207